Kinetic Characterization of Human Histone Deacetylase 8 With Medium-Chain Fatty Acyl Lysine

Harrison Yoo and Gregory A Polsinelli

Department of Pharmaceutical and Administrative Sciences, University of Charleston School of Pharmacy, Charleston, WV, USA.

Epigenetics Insights
Volume 14: 1–6

DOI: 10.1177/25168657211065685

SAGE

ABSTRACT: Histone deacetylases (HDACs) catalyze the removal of ε-acetyl-lysine residues of histones via hydrolysis. Removal of acetyl groups results in condensation of chromatin structure and alteration of gene expression by repression. HDACs are considered targets for the treatment of cancer due to their role in regulating transcription. HDAC8 inhibition may be an important anti-proliferative factor for histone deacetylase inhibitors on cancer cells and may give rise to the progression of apoptosis. HDAC8 activity was analyzed with various peptides where the target lysine is modified with medium-chain fatty acyl group. Kinetic data were determined for each p53 peptide substrate. The results suggest that there was HDAC8 deacetylase activity on peptide substrate as well as deacylase activity with acylated peptide substrate variants. HDAC8 inhibition by hexanoic and decanoic acid was also examined. The K_i for hexanoic and decanoic acid were determined to be 2.35 ± 0.341 and 4.48 ± 0.221 mM, respectively.

KEYWORDS: HDAC8, cancer, epigenetics, enzymology, deacylase, lysine modification

RECEIVED: September 24, 2021. **ACCEPTED:** November 19, 2021.

TYPE: Original Research

FUNDING: The author(s) disclosed receipt of the following financial support for the research, authorship, and/or publication of this article: This research was funded by NIH Grant P20GM103434 to the West Virginia IDeA Network for Biomedical Research Excellence (WV-INBRE).

DECLARATION OF CONFLICTING INTERESTS: The author(s) declared no potential conflicts of interest with respect to the research, authorship, and/or publication of this article.

CORRESPONDING AUTHOR: Gregory A Polsinelli, Department of Pharmaceutical and Administrative Sciences, University of Charleston School of Pharmacy, 2300 MacCorkle Avenue, SE, Charleston, WV, 25304 USA. Email: gregorypolsinelli@ucwv.edu

Introduction

Acetyl groups of histone tails are removed by histone deacetylases (HDACs), while histones are acetylated by histone acetyltransferases (HATs). Deacetylation of histones results in condensation of chromatin structure and repression of gene expression. Decreases in acetylated histone causes silencing of the affected genes and hence, this is linked to development of cancer. Because of this, HDACs increasingly have become significantly important targets for the treatment of cancers.[1] There are currently several HDAC inhibitors that are undergoing various clinical trial stages to be approved by the Food and Drug Administration (FDA), while several drugs are already approved by the FDA such as vorinostat (suberoylanilide hydroxamic acid or SAHA) and romidepsin. These 2 drugs are approved with indication of cutaneous T cell lymphoma treatment.[2] Belinostat, panabiostat, and valproic acid, a short-chain branched fatty acid, have also been approved for various disorders.[3] Studies have also shown inhibition of growth of human lung, colon, and cervical cancer cell lines where HDAC8 has been knocked down.[4]

There are 4 classes of histone deacetylases. Human class I, II, and IV HDACs are said to be zinc-dependent in that they require divalent zinc ions to catalyze the deacetylase reaction. Class I HDACs include HDAC1, -2, -3, and -8. These are homologs of yeast RPD3.[5,6] HDACs 1-3 require association with large multisubunit corepressor complexes and are considered inactive by themselves. HDAC8 is fully active in and of itself and is the only extensively kinetically characterized HDAC.[7-10] HDAC3 was also recently characterized.[11] Class II HDACs are subclassified as class IIa (HDAC4, -5, -7, and -9) and class IIb (HDAC6 and -10) and are homologs of yeast HDA1 protein.[6,12] All members of class IIa can shuttle between the nucleus and cytoplasm. The only class IV deacetylase is HDAC11.[13] It is a homolog of yeast HOS3. Class III HDACs are NAD(+)-dependent and are referred to as sirtuins.[14] This class of HDAC share no sequence similarity with class I and II HDACs and use a different catalytic mechanism.[15]

The crystal structures of HDAC3 and -8 show that each bind 2 monovalent cations (MVCs), likely Na^+ or K^+, in addition to the catalytic divalent metal ion.[4,10,16,17] The 2 MVC binding sites have been designated as site 1 and site 2 with site 1 located approximately 7 Å from the divalent catalytic center and site 2 is ⩾20 Å from the divalent metal center.[4,17] The crystal structures of other class I and II human HDACs also bind K^+ at these same sites in addition to bacterial histone deacetylase-like amidohydrolase.[18-20] A study on the effects of varying concentrations of Na^+ or K^+ on catalysis of HDAC3[11] and HDAC8[8] have been reported. Na^+ concentration was shown to have little effect on catalysis of HDAC8 while a greater effect on catalysis of HDAC8 was observed with potassium.

The crystal structure of HDAC3/SMRT displays an active site Zn(II) and a channel leading to it that is likely obstructed in absence of NCOR1, or SMRT.[17] However, based on observations of the crystal structure of HDAC8, this channel leading into the Zn(II) active site is always open, which offers explanation for its activity by itself.[4] It also has been determined that ethylenediamine tetra-acetic acid (EDTA) can be used to chelate Zn(II) ions of HDAC8 forming apo-HDAC8 and its activity can be recovered by adding Zn(II), Fe(II), or Co(II).[7] Also, it was shown that HDAC8 activity was greater with Fe(II)-HDAC8 and Co(II)-HDAC8 and that excess Zn(II) inhibits HDAC8 activity.

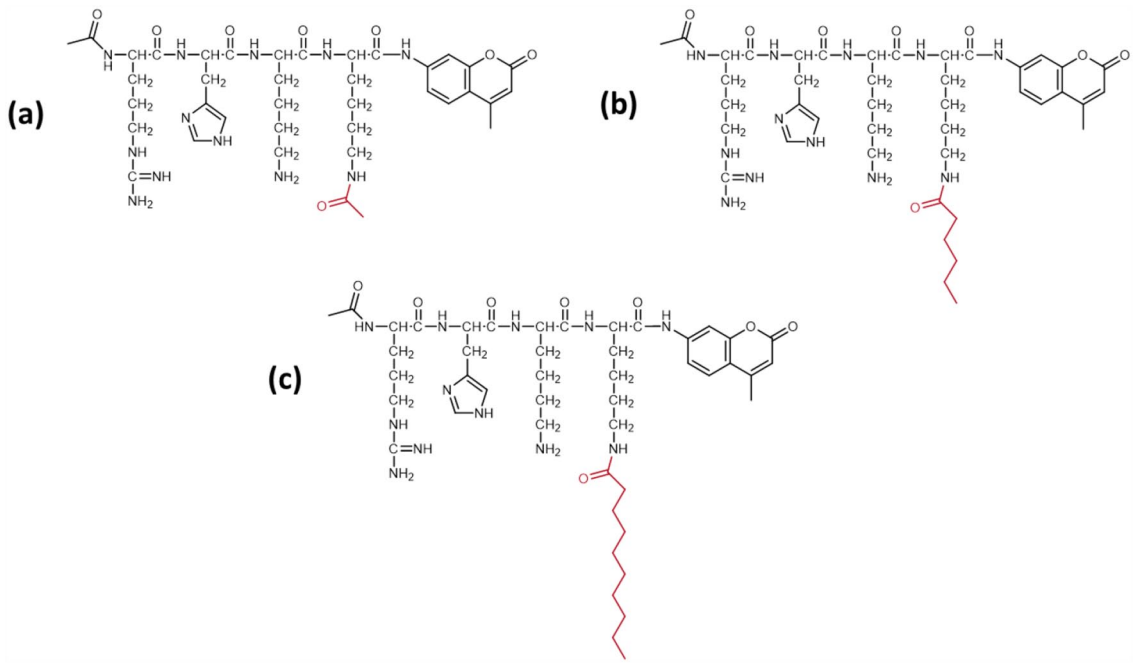

Figure 1. Structures of peptide substrates with AMC (7-amino-4-methylcoumarin) fluorophore-coupled substrates screened for HDAC8 deacylase activity showing differentially modified lysines (red). The peptide sequence RHKK is based on the physiological substrate (p53 379-382) for SIRT1. (a) AcRHKK(acetyl)-AMC is the standard physiological substrate deacetylated by HDAC8, (b) AcRHKK(hex)-AMC, and (c) AcRHKK(dec)-AMC.

The current goal of this study is to carry out enzyme kinetic studies to determine HDAC8 deacetylase and deacylase activity with peptide substrate as well as activity of HDAC8 with differentially acylated lysine residues. It has been reported that SIRT5,[21-23] and SIRT2[24] and SIRT6[25,26] are able to deacylate long chain fatty acylated lysines. The same has been reported for HDAC1, -2,-3,[27] HDAC8,[28] and HDAC11.[27-29] Little to no activity was reported for HDAC8 with regard to its ability to deacylate short-, medium-, and long-chain fatty acylated lysine when compared to the nonphysiologically relevant trifluoracetylated lysine substrate.[27] HDAC11 has been shown to deacylate short- and medium chain fatty acyl lysine.[29] In the present study, the kinetic characterization and identification of HDAC8 activity with different peptide substrates will provide invaluable insight for the design of HDAC8-specific inhibitors. The present study seeks to determine the effects of medium-chain fatty acylated lysine on catalytic activity of HDAC8. The results from this study demonstrate that medium-chain fatty acylated lysines (typically categorized as C6-C10) are deacylated by HDAC8. We also report the inhibition constants (K_i) of hexanoic and decanoic acid for HDAC8.

Results and Discussion

Kinetic characterization of HDAC8 with medium chain fatty acyl lysine

HDAC8 was reacted with AcRHKK(acetyl)-AMC, AcR HKK(hex)-AMC, and AcRHKK(dec)-AMC (Figure 1). 1 μM HDAC8 was mixed with various concentrations of compounds shown in Figure 1 and stopped at various time points as described below. The data were plotted using GraphPad Prism to determine K_M, k_{cat}, and k_{cat}/K_M values. Michaelis-Menten plots are shown in Figure 2 and the kinetic constants are tabulated in Table 1 calculated using the Michaelis-Menten equation. Based on the data in Figure 2 and Table 1, a 2-fold increase in catalytic activity (k_{cat}/K_M) is observed for AcRHKK(hex)-AMC in comparison to AcRHKK(acetyl)-AMC. A 3-fold increase in catalytic activity is observed for AcRHKK(dec)-AMC versus AcRHKK(acetyl)-AMC. This data is similar to that previously determined for long-chain fatty acylated lysines where different peptide substrate was used.[28] The K_M value decreased as the acyl group on the lysine of the peptide substrate increased in length suggesting tighter binding of substrate and thereby increasing catalytic efficiency.

HDAC8 inhibition by hexanoic and decanoic fatty acids

Inhibition of HDACs by fatty acids have been a focus of study recently.[11,29,30] For this reason, in addition to an interest in the possibility of product inhibition at high concentrations of substrate in Figure 2b and c, a study of HDAC8 inhibition by hexanoic and decanoic acid was undertaken. Varying concentrations of fatty acid (hexanoic and decanoic acids) were preincubated with 1 μM HDAC8 for at least 10 minutes and 1 μM AcRHKK(acetyl)-AMC was added as substrate to initiate the reactions. The inhibition constants (K_i; Table 2) were determined by plotting fractional activity versus concentration of fatty acid and fitted the data using equation (1) (Figure 3). The K_i for hexanoic acid was determined to be 2.35 mM while

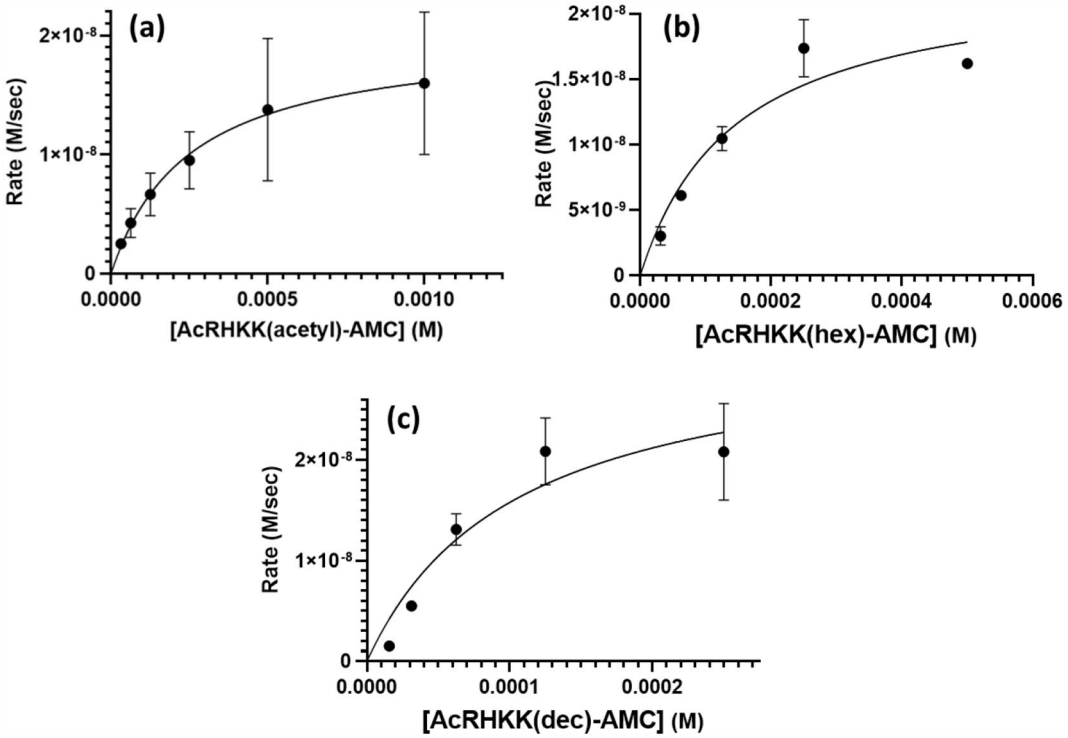

Figure 2. Michaelis-Menten plots of rate (M/second) versus concentration of substrate peptide (M) with standard deviation error bars. 1 μM HDAC8 was mixed with varying concentrations of each substrate in 25 mM Tris pH 8.0, 10 mM KCl with 500 μM EDTA (free acid) at room temperature. (a) AcRHKK(acetyl)-AMC, (b) AcRHKK(hex)-AMC, and (c) AcRHKK(dec)-AMC. Kinetic data are reported in Table 1. For panels (a-c), each experiment was completed in duplicate.

Table 1. Reactivity of HDAC8 (±SD) with medium-chain fatty acylated lysine.[a]

PEPTIDE SUBSTRATE	K_{CAT} (S^{-1})	K_M (M)	K_{CAT}/K_M (M^{-1} S^{-1})
AcRHKK(acetyl)-AMC	0.0201 ± 0.00930	0.000251 ± 7.75 × 10^{-5}	80.1 ± 12.3
AcRHKK(hex)-AMC	0.0230 ± 3.54 × 10^{-5}	0.000146 ± 2.51 × 10^{-5}	158.0 ± 26.5
AcRHKK(dec)-AMC	0.0322 ± 0.00906	0.000104 ± 2.50 × 10^{-5}	309.1 ± 12.3

[a]HDAC8 was assayed as described below. Steady-state kinetic parameters were determined from a fit of the Michaelis-Menten equation to the dependence of the initial rate on the substrate concentration at 1 μM HDAC8 from Figure 2.

that of decanoic acid was determined to be 4.48 mM. Hexanoic acid is approximately 2-fold more potent as an inhibitor of HDAC8 than decanoic acid.

The possibility of micelle formation by hexanoic and decanoic acid has also been considered. Hexanoic acid is generally considered to have a critical micelle concentration (CMCs) of 29.3 mM which is above the ranges used in Figure 3a. Several different CMCs have been reported for decanoic acid with 28 mM being the lowest reported value and 102 mM the highest.[31-33] It is therefore unlikely that micelle formation interfered with the assay conditions below these reported CMC values. In fact, micelle formation by decanoic acid would likely have caused less inhibition at concentrations above its CMC. In Figure 3b, approximately 99% inhibition is observed above 20 mM decanoic acid.

HDAC8 docking studies

Docking calculation studies were completes using Chem3D with AutoDock interface to position RHKK(hex) and RHKK(dec) substrates within the active site of HDAC8 (PDB: 5D1B) (Figure 4a and b).[34] Docking simulations were carried out using the zinc ion (green; Figure 4) as the centroid of the selection with atoms within 14 Å of the active site Zn(II) selected. The active site zinc was assigned a formal charge of +2. Trichostatin A (TSA) and glycerols bound at the active site in

Table 2. Inhibition of HDAC8 (±SD) by hexanoic and decanoic acid.[a]

INHIBITOR	K_i (mM)
Hexanoic acid	2.35 ± 0.341
Decanoic acid	4.48 ± 0.221

[a]HDAC8 inhibition by hexanoic and decanoic acid was assayed as described below. Inhibition constants (K_i) were determined by fitting equation (1) to the data in Figure 3.

the original crystal structure were deleted prior to docking calculations. The most plausible positioning of peptide substrate for RHKK(hex) and RHKK(dec) are shown in Figure 4a and b, respectively. For RHKK(hex), the positioning with the most favorable binding energy out of 20 positionings is shown in Figure 4a. The calculated free energy of binding ($\Delta G_{binding}$) was calculated to be −3.67 kcal/mol. For RHKK(dec), the positioning with the most favorable binding energy out of twenty positionings is shown in Figure 4b. The calculated free energy of binding ($\Delta G_{binding}$) was calculated to be +3.48 kcal/mol. All binding energies calculated for the 20 positionings of RHKK(dec) in HDAC8 were positive though a positive $\Delta G_{binding}$ is common when docking larger compounds. As shown in Figure 3b, $\Delta G_{binding}$ should be negative as binding and inhibition does occur based on this in vitro data. In both docking results, the fatty acyl amido oxygen and nitrogen are positioned to complex with the zinc ion of the HDAC8 active site as expected. The remainder of the fatty acyl chain is positioned within the channel comparable to the lateral tunnel (or foot pocket or acetate release channel) previously reported[29,35,36] for both RHKK(hex) and RHKK(dec). RHKK(hex) and RHKK(dec) was positioned within HDAC8 with the fatty acyl chain bound inside the vertical tunnel but with higher calculated binding energy.

Docking calculations for binding of hexanoic (Figure 4c) and decanoic (Figure 4d) acid inhibitors were also completed. Figure 4c and d show the 20 most energetically favorable positionings of each fatty acid within HDAC8. All binding energy calculations for the 20 positions of hexanoic acid within HDAC8 (Figure 4c) were favorable and ranged from −2.78 to −3.17 kcal/mol. All binding energy calculations for the 20 positions of decannoic acid within HDAC8 (Figure 4d) were favorable and ranged from −3.75 to −4.68 kcal/mol. For both hexanoic and decanoic acids, the positions calculated were almost exclusively within the lateral tunnel (or foot pocket) of HDAC8. Otherwise, they were positioned in the HDAC8 active site or active site tunnel. The carboxylate group in each case was not positioned in complex with the active site zinc.

Materials and Methods

Materials

All peptides were synthesized by GenScript with >95% purity determined by HPLC-MS. Hexanoic acid (≥95%) was purchased from Acros Organics. Decanoic acid (≥95%) was purchased from Tokyo Chemical Industry. >90% purity (by SDS-PAGE) human HDAC8 His-Tag in 25 mM HEPES pH 7.5, 300 mM NaCl, 5% glycerol, 0.04% triton X-100, and 0.2 mM TCEP was purchased from Active Motif. Enzyme came from the same lot number (lot # 32016001). The recombinant enzyme consists of full length human HDAC8 (accession number NP_060956.1) with an N-terminal 6xHis tag expressed in a baculovirus expression system. All buffers used in this study were treated with chelex resin prior to use in the enzyme assays.

Metal-free Apo-HDAC8 preparation

≥90% pure HDAC8 was prepared by dialyzing against 25 mM MOPS, 10 µM dipicolinic acid, and 1mM EDTA at pH 7.0 overnight with 2 exchanges of buffer followed by overnight dialysis with 25 mM MOPS at pH 7.5 without EDTA. HDAC8 was reconstituted with enzyme dilution buffer consisting of 25 mM Tris at pH 8.0, 1 mM NaCl, 10 mM KCl, and 2.34 µM $ZnCl_2$ and incubating on ice for 1 hour.

HDAC8 activity assay

The deacylase/deacetylase activity of HDAC8 was measured using the commercially available Fluor de Lys HDAC8 assay kit from Enzo Life Sciences as previously described.[7,8,11,27] Briefly, the assay uses a fluorophore-coupled method for indirectly determining deacylation/deacetylation of lysine peptide substrate by employing an AMC (7-amino-4-methylcoumarin) label (Figure 1a-c) that is protected while the adjacent lysine is still acylated/acetylated. After deacylation/deacetylation, the AMC label is cleaved using a developer solution. Enzyme assays were performed in 96-well plates and reactions were stopped at varying time points using Developer II solution containing 1 µM TSA (an HDAC8 inhibitor).[34] AMC fluorescence as an indicator of deacetylation/deacylation was measured using a Tecan 96-well plate reader with excitation and emission wavelengths of 360 and 460 nm, respectively. The concentration of product at each time point was calculated from a standard curve prepared using solutions containing known concentrations of the AMC product (0-40 µM). Except for the inhibition study, all assays were performed in at least duplicate and in 25 mM Tris pH 8.0, 10 mM KCl with 500 µM EDTA (free acid) at room temperature.

For medium-chain fatty acid inhibition assays, varying concentrations of fatty acid (hexanoic and decanoic acids) were pre-incubated with 1 µM HDAC8 for at least 10 minutes and 1 µM AcRHKK(acetyl)-AMC was added as substrate to initiate the reactions. In all assays, the final NaCl concentration contributed by the enzyme storage buffer is ≤6 mM. The inhibition constant (K_i) was determined by plotting fractional activity versus [fatty acid] and fitting the data using equation (1).

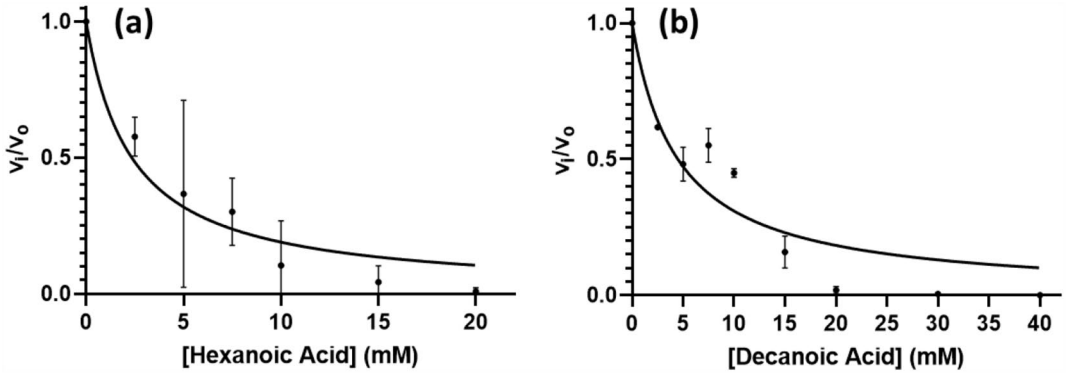

Figure 3. Inhibition of HDAC8 by hexanoic (a) and decanoic acid (b) with standard deviation error bars. 1 μM HDAC8 was pre-incubated for at least 10 minutes with varying concentrations of either hexanoic or decanoic acid in 25 mM Tris pH 8.0, 10 mM KCl with 500 μM EDTA (free acid) and then mixed with 1 μM AcRHKK(acetyl)-AMC as substrate at room temperature. Initial velocities were determined from fluorescence changes over time, normalized, plotted versus hexanoic (a) or decanoic acid (b) concentration, and fitted using equation (1). For panel (a), each data point was performed in triplicate except for the 2.5 mM point which was performed in duplicate. For panel (b), the 30 mM data point was measured in triplicate while all other data points were performed in duplicate. Inhibition constants for each are reported in Table 2.

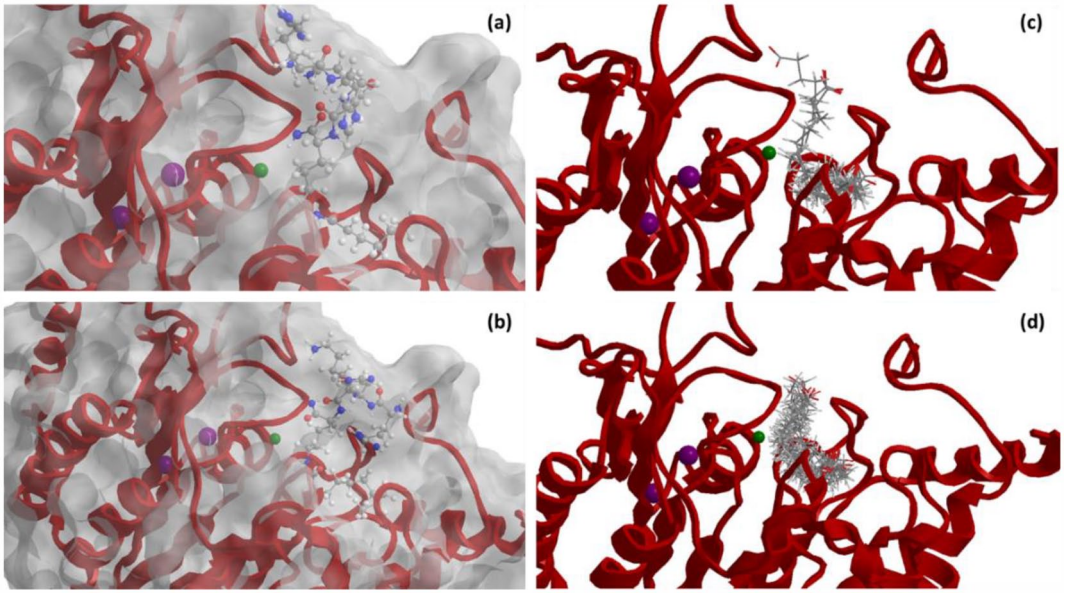

Figure 4. AutoDock results for HDAC8 (PDB: 5D1B, red ribbon)[34] docked with RHKK(hex) (panel (a)), RHKK(dec) (panel (b)), hexanoic (panel (c)) and decanoic (panel (d)) fatty acids. Panel (a): RHKK(hex) substrate is shown in ball-and-stick configuration. Panel (b): RHKK(dec) substrate is shown in ball-and-stick configuration. Panel (c): the top 20 most energetically favorable positioning of hexanoic acid inhibitor is shown in stick configuration. Panel (d): the top 20 most energetically favorable positioning of decanoic acid inhibitor is shown in stick configuration. Color scheme for peptide substrate and fatty acid inhibitors: red = oxygen; blue = nitrogen; gray = carbon; white = hydrogen. Two bound potassium ions are shown in purple.

$$\frac{v_i}{v_o} = \frac{V_{max}}{1 + \frac{[I]}{K_i}} \quad (1)$$

Data analysis for all kinetic and inhibition data was performed using GraphPad Prism 12.0. Each experiment, whether completed in duplicate or triplicate, was performed as a separate trial with error bars shown in Figures 2 and 3 generated by the GraphPad Prism 12.0 software. Numerical ranges of the standard deviation error bars are shown in Tables 1 and 2.

HDAC8 docking studies

Docking experiments showing HDAC8 (PDB: 5D1B, red)[34] docked with RHKK(hex), RHKK(dec), hexanoic and decanoic fatty acids. Experiments were performed using Chem3D with AutoDock interface.[37,38] Docking simulations were carried out using the zinc ion as the centroid of the selection with atoms within 14 Å of the active site Zn(II) selected. The active site zinc was assigned a formal charge of +2. TSA bound at the active site in the original crystal structure was deleted. RHKK(hex) and RHKK(dec) were docked using X, Y, and Z

number of grid points set to 60 where the spacing of grids was set to 0.375 Å. Hexanoic and decanoic acid were docked using X, Y, and Z number of grid points set to 40 where the spacing of grids was set to 0.375 Å.

Conclusions

HDAC8 had activity with physiological peptide substrate (AcRHKK(acetyl)-AMC) based on p53 sequence. AcRHKK(dec)-AMC had the highest catalytic reaction efficiency per quantity substrate assayed with the highest k_{cat}/K_M among substrates tested. Hexanoic acid exhibited greater HDAC8 inhibition compared to decanoic acid with a K_i that is approximately 1-half of that determined for decanoic acid. Further HDAC8 studies of enzyme kinetics will help elucidate additional features that are unique to HDAC8, allowing for the development of HDAC8-specific inhibitors as cancer therapeutics. Little is known about the role of HDAC8 and p53 deacetylation or deacylation which supports the significance of the in vitro and in silico data reported here. When p53 is acetylated, it is more stable and can therefore inhibit tumor growth through induction of cell cycle arrest and/or apoptosis.[39] Future experiments will include cell culture experiments to further test for in vivo inhibitory activity of hexanoic and decanoic acid and further validate in silico docking results reported here.

Author Contributions

Conceptualization, G.A.P.; methodology, G.A.P.; formal analysis, H.Y. and G.A.P.; data curation, H.Y. and G.A.P.; writing—original draft preparation, H.Y. and G.A.P.; writing—review and editing, H.Y. and G.A.P.; supervision, G.A.P.; project administration, G.A.P.; funding acquisition, G.A.P.

ORCID iD

Gregory A Polsinelli https://orcid.org/0000-0002-7681-5770

REFERENCES

1. Marks PA, Breslow R. Dimethyl sulfoxide to vorinostat: development of this histone deacetylase inhibitor as an anticancer drug. *Nat Biotechnol*. 2007;25:84-90.
2. Wagner JM, Hackanson B, Lübbert M, Jung M. Histone deacetylase (HDAC) inhibitors in recent clinical trials for cancer therapy. *Clin Epigenetics*. 2010;1:117-136.
3. Eckschlager T, Plch J, Stiborova M, Hrabeta J. Histone deacetylase inhibitors as anticancer drugs. *Int J Mol Sci*. 2017;18:1414.
4. Vannini A, Volpari C, Filocamo G, et al. Crystal structure of a eukaryotic zinc-dependent histone deacetylase, human HDAC8, complexed with a hydroxamic acid inhibitor. *Proc Natl Acad Sci USA*. 2004;101:15064-15069.
5. Taunton J, Hassig CA, Schreiber SL. A mammalian histone deacetylase related to the yeast transcriptional regulator Rpd3p. *Science*. 1996;272:408-411.
6. Rundlett SE, Carmen AA, Kobayashi R, Bavykin S, Turner BM, Grunstein M. HDA1 and RPD3 are members of distinct yeast histone deacetylase complexes that regulate silencing and transcription. *Proc Natl Acad Sci USA*. 1996;93:14503-14508.
7. Gantt SL, Gattis SG, Fierke CA. Catalytic activity and inhibition of human histone deacetylase 8 is dependent on the identity of the active site metal ion. *Biochemistry*. 2006;45:6170-6178.
8. Gantt SL, Joseph CG, Fierke CA. Activation and inhibition of histone deacetylase 8 by monovalent cations. *J Biol Chem*. 2010;285:6036-6043.
9. Gantt SM, Decroos C, Lee MS, et al. General base-general acid catalysis in human histone deacetylase 8. *Biochemistry*. 2016;55:820-832.
10. Dowling DP, Gattis SG, Fierke CA, Christianson DW. Structures of metal-substituted human histone deacetylase 8 provide mechanistic inferences on biological function. *Biochemistry*. 2010;49:5048-5056.
11. Polsinelli GA, Yu HD. Regulation of histone deacetylase 3 by metal cations and 10-hydroxy-2E-decenoic acid: possible epigenetic mechanisms of queen-worker bee differentiation. *PLoS One*. 2018;13:e0204538.
12. Carmen AA, Rundlett SE, Grunstein M. HDA1 and HDA3 are components of a yeast histone deacetylase (HDA) complex. *J Biol Chem*. 1996;271:15837-15844.
13. Gao L, Cueto MA, Asselbergs F, Atadja P. Cloning and functional characterization of HDAC11, a novel member of the human histone deacetylase family. *J Biol Chem*. 2002;277:25748-25755.
14. Moazed D. Enzymatic activities of Sir2 and chromatin silencing. *Curr Opin Cell Biol*. 2001;13:232-238.
15. Blander G, Guarente L. The Sir2 family of protein deacetylases. *Annu Rev Biochem*. 2004;73:417-435.
16. Somoza JR, Skene RJ, Katz BA, et al. Structural snapshots of human HDAC8 provide insights into the class I histone deacetylases. *Structure*. 2004;12:1325-1334.
17. Watson PJ, Fairall L, Santos GM, Schwabe JW. Structure of HDAC3 bound to co-repressor and inositol tetraphosphate. *Nature*. 2012;481:335-340.
18. Nielsen TK, Hildmann C, Dickmanns A, Schwienhorst A, Ficner R. Crystal structure of a bacterial class 2 histone deacetylase homologue. *J Mol Biol*. 2005;354:107-120.
19. Bottomley MJ, Lo Surdo P, Di Giovine P, et al. Structural and functional analysis of the human HDAC4 catalytic domain reveals a regulatory structural zinc-binding domain. *J Biol Chem*. 2008;283:26694-26704.
20. Schuetz A, Min J, Allali-Hassani A, et al. Human HDAC7 harbors a class IIa histone deacetylase-specific zinc binding motif and cryptic deacetylase activity. *J Biol Chem*. 2008;283:11355-11363.
21. Du J, Zhou Y, Su X, et al. Sirt5 is a NAD-dependent protein lysine demalonylase and desuccinylase. *Science*. 2011;334:806-809.
22. Peng C, Lu Z, Xie Z, et al. The first identification of lysine malonylation substrates and its regulatory enzyme. *Mol Cell Proteomics*. 2011;10:M111.012658.
23. Tan M, Peng C, Anderson KA, et al. Lysine glutarylation is a protein posttranslational modification regulated by SIRT5. *Cell Metab*. 2014;19:605-617.
24. Teng YB, Jing H, Aramsangtienchai P, et al. Efficient demyristoylase activity of SIRT2 revealed by kinetic and structural studies. *Sci Rep*. 2015;5:8529.
25. Jiang H, Khan S, Wang Y, et al. SIRT6 regulates TNF-α secretion through hydrolysis of long-chain fatty acyl lysine. *Nature*. 2013;496:110-113.
26. Feldman JL, Baeza J, Denu JM. Activation of the protein deacetylase SIRT6 by long-chain fatty acids and widespread deacylation by mammalian sirtuins. *J Biol Chem*. 2013;288:31350-31356.
27. Moreno-Yruela C, Galleano I, Madsen AS, Olsen CA. Histone Deacetylase 11 Is an ε-N-Myristoyllysine hydrolase. *Cell Chem Biol*. 2018;25:849-856.e8.
28. Aramsangtienchai P, Spiegelman NA, He B, et al. HDAC8 catalyzes the hydrolysis of long chain fatty acyl lysine. *ACS Chem Biol*. 2016;11:2685-2692.
29. Kutil Z, Novakova Z, Meleshin M, Mikesova J, Schutkowski M, Barinka C. Histone Deacetylase 11 Is a fatty-acid deacylase. *ACS Chem Biol*. 2018;13:685-693.
30. Spannhoff A, Kim YK, Raynal NJ, et al. Histone deacetylase inhibitor activity in royal jelly might facilitate caste switching in bees. *EMBO Rep*. 2011;12:238-243.
31. Kimura Y, Hosoda Y, Shima M, Adachi S, Matsuno R. Physico-chemical properties of fatty acids for assessing the threshold concentration to enhance the absorption of a hydrophilic substance. *Biosci Biotechnol Biochem*. 1998;62:443-447.
32. Medoš, Bešter-Rogač M. Thermodynamics of the micellization process of carboxylates: a conductivity study. *J Chem Thermodyn*. 2015;83:117-122.
33. Rodriguez M, Funke S, Fink M, et al. Plasma fatty acids and [^{13}C]linoleic acid metabolism in preterm infants fed a formula with medium-chain triglycerides. *J Lipid Res*. 2003;44:41-48.
34. Decroos C, Christianson NH, Gullett LE, et al. Biochemical and structural characterization of HDAC8 mutants associated with Cornelia de Lange syndrome spectrum disorders. *Biochemistry*. 2015;54:6501-6513.
35. Wang DF, Wiest O, Helquist P, Lan-Hargest HY, Wiech NL. On the function of the 14 A long internal cavity of histone deacetylase-like protein: implications for the design of histone deacetylase inhibitors. *J Med Chem*. 2004;47:3409-3417.
36. Whitehead L, Dobler MR, Radetich B, et al. Human HDAC isoform selectivity achieved via exploitation of the acetate release channel with structurally unique small molecule inhibitors. *Bioorg Med Chem*. 2011;19:4626-4634.
37. Morris GM, Huey R, Lindstrom W, et al. AutoDock4 and AutoDockTools4: automated docking with selective receptor flexibility. *J Comput Chem*. 2009;30:2785-2791.
38. Huey R, Morris GM, Olson AJ, Goodsell DS. A semiempirical free energy force field with charge-based desolvation. *J Comput Chem*. 2007;28:1145-1152.
39. Tang Y, Zhao W, Chen Y, Zhao Y, Gu W. Acetylation is indispensable for p53 activation. *Cell*. 2008;133:612-626.